

Article

Groundwater-Sewer Interaction in Urban Coastal Areas

Ting Liu [†] , Xin Su [†] and Valentina Prigiobbe ^{*}

Department of Civil, Environmental, and Ocean Engineering, Stevens Institute of Technology, Hoboken, NJ 07030, USA; tliu18@stevens.edu (T.L.); xsu1@stevens.edu (X.S.)

^{*} Correspondence: valentina.prigiobbe@stevens.edu; Tel.: +1-201-216-5310

[†] These authors contributed equally to this work.

Received: 4 November 2018 ; Accepted: 22 November 2018 ; Published: 3 December 2018



Abstract: In this paper, a study of the potential causes of the occurrence of high concentration of *Enterococcus Faecalis* in surface water within urban areas in dry-weather conditions (DWCs) is presented. Two hypotheses were formulated: (1) undersized sewer system; and (2) groundwater infiltration into damaged sewer pipes. In both cases, more frequent combined sewer overflows (CSOs) may occur discharging untreated sewage into surface water. To evaluate the first hypothesis, a hydraulic model of a sewer was developed assuming a water-tight system. The simulation results show that CSOs never occur in DWCs but a rain event of intensity equal to 1/3 of one-year return period may trigger them. To evaluate the second hypothesis, a model combining sewer failure with groundwater level was developed to identify the sections of damaged sewer below the water table and, therefore, potentially affected by infiltration. The risk of infiltration exceeds 50% in almost half of the entire network even at the lowest calculated water table. Considering 50% of infiltration distributed throughout that part of the network, CSOs can occur also in DWCs.

Keywords: coastal cities; groundwater; infiltration; infrastructure; sewer; urban hydrology

1. Introduction

Since more than half of the global population resides in urban settings, providing safe, reliable water to city populations is a challenge that defines the 21st century [1]. In the U.S. alone, the share of urban residents has already grown to 80%, with the world population projected to increase of 70% by 2050. Even in less developed countries, the majority of people will be living in urban areas [2,3]. Urban surface water and groundwater may be increasingly required (or desired) as an alternative to conventional, but less available, pristine water [4,5]. Therefore, the water quality should be preserved by preventing contamination [6–8]. One of the major stressors on natural urban water is the discharge of untreated sewage containing toxic and pathogenic contaminants into natural water bodies, which cause a variety of diseases including diarrhea, the leading cause of illness and death on a global basis [9]. Combined sewer overflows (CSOs) are one of the major causes of uncontrolled discharges of untreated sewage during wet-weather conditions (WWCs). Studies of the impact of sewage overflows on coastal water have shown that the discharge of wastewater can significantly contribute to the accumulation of micro-pollutants (e.g., personal-care products and pharmaceuticals), fecal bacteria, and viruses in the near-shore water and on the sediments, which negatively affect the water quality and present health risks for the population [10–13]. Events of urban disruption and contamination due to sewer overflows are occurring more frequently [14–18], suggesting the emergence of a serious problem in big or rapidly growing cities. The study by Young et al. [15] reports the occurrence of the antibiotic-resistant bacteria (heterotrophic bacteria resistant to tetracycline and ampicillin) in the Hudson River Estuary near New York City metropolitan area and they ascribed presence of the high concentration of these contaminants to CSOs. Similar observations were made by

Edge and Hill [19], McLellan et al. [17], Donovan et al. [20], and Morgan et al. [18] who studied other urban waterways.

In the United States, according to the U.S. EPA report [21], the majority of the current underground utility infrastructure was built after World War II, making the average age of sewer systems in the U.S. more than 40 years old. On the eastern part of the U.S., sewer systems are even almost 200 years old. According to the American Waterworks Association (AWWA) industry database, there are approximately 1,483,000 km of municipal water piping in the U.S., making sewer replacement and rehabilitation the most capital intensive issue in urban drainage [22]. Pipes have a lifetime that can range from 15 to over 100 years varying considerably depending on soil conditions, pipe material, climate, and capacity requirements. The U.S. EPA forecasts that by 2020 approximately 23% of the sewer system will be in a very poor condition. Structural damages make the pipe pervious and potentially affected by infiltrations of groundwater [23–28]. The consequences of the infiltration are: the dilution of the wastewater with consequent malfunction of the wastewater treatment plant (WWTP) units [29–31], the erosion of the soil surrounding the pipe with loss of supporting strength [32], and more frequent CSOs with the discharge of untreated wastewater into surface water bodies [23,33].

Enterococci Faecalis are Fecal Indicator Bacteria (FIB) whose determination is recommended by the U.S. EPA to monitor sewage contamination in waterways [34–36]. Their concentration in waterways near some of the most populated areas in the U.S. can exceed the EPA guidelines for water quality after a minor rain event, or even unexpectedly in dry-weather conditions. Documented cases in the U.S. are along, e.g., the Malibu Coastline (CA) near Los Angeles [37], the coastline in Santa Barbara (CA) [38], the Delaware River within Philadelphia [39], the Charles River within Boston [40], and the estuary of the Hudson River near New York City [41]. Similar observations were made in, e.g., Australia [42], China [43], Germany [44], Mexico [45], and UK [46]. Two hypotheses are formulated to explain the observed large concentrations of FIB. The first hypothesis proposes that the sewer system is undersized. The second hypothesis states that groundwater infiltrates into damaged sewer pipes. In both cases, more frequent CSOs may occur, with discharge of contaminants into surface water bodies [10–13]. Wolf et al. [47] studied the groundwater–sewer interaction in the City of Rastatt (Germany). They combined a sewer defect database and hydrogeological information to understand the potential negative impact of leakage (or exfiltration) of damaged sewer pipes. Recently, Yap and Ngien [31] estimated the amount of infiltration and inflow to be between 17% and 21% of the flow. This parasitical water reduced the capacity of the sewer pipes and increased the inflow to sewerage treatment plant. The work by Wittenberg and Aksoy [26] shows that intruded groundwater flows show recessions and seasonal variations correlated to baseflow in neighboring rivers. Therefore, it is critical to account for the natural surface water bodies nearby the sewer system of interest.

In this paper, the two hypotheses listed above were analyzed on a selected urban catchment of the City of Hoboken (NJ). To evaluate the first hypothesis, a hydraulic model of sewer flow was implemented assuming a water-tight system. To test the second one, a model combining sewer failure with a groundwater level was developed to calculate the risk of infiltration of sewer sections under various conditions of the water table.

2. Material and Methods

Sewer and groundwater flow simulations in conjunction with the determination of risk of failure and infiltration were performed with the model described in this section. Simulations using a hydrologic model of the sewer flow in dry weather were run to verify the first hypothesis regarding the FIB events in DWCs, i.e., the sewer network is undersized and therefore there are CSOs in DWCs. Then, simulations to determine the groundwater table were run. Upon the assessment of the damaged pipes across the network using a failure model, the results of the groundwater flow model were used to compute the risk of infiltration. Finally, considering the sections of the sewer at high risk of infiltration, sewer flow simulations were carried out and the minimum level of infiltration required for the CSOs to occur in DWCs was determined.

2.1. Study Area

The city of Hoboken was chosen as urban laboratory because of its geographical location along a coast, its compact urban structure, accessible natural water systems, documented problems of groundwater infiltration into the sewer system by the local Water Authority, and dry-weather FIB events. Figure 1 shows the FIB concentrations as a function of rainfall four days prior the measurements for locations at the estuary of the Hudson River, namely, in the City of Hoboken (NJ) and in New York City (NYC). The Rainfall 4 Days Prior indicates the total rain four days prior to the FIB concentration measurement.

Hoboken is located in northeast New Jersey and has a land area of approximately 3 km² with approximately 53,635 inhabitants [48]. The land use of the city is predominantly urban with some greenspace and open ground. The city is bounded on the east by the Hudson River and on the west by steep slopes upwards leading to Jersey City heights. Lidar data from New Jersey Department of Environmental Protection (NJDEP) were used to identify the topography of the area and the street elevations [49]. The topography of the modeled area ranges between 0.5 and 30.7 m (i.e., between 1.8 and 100.7 ft) based on North American Vertical Datum of 1988 (NAVD 88). Hoboken is predominantly underlain by the Stockton rock formation with significant portions of Serpentine and Manhattan Schist in the regions bordering the Hudson River. The more superficial soil consists of rahway-till, deltaic, and estuarine/salt-marsh deposits with some outcrops of fractured bedrock (i.e., fractured serpentine).

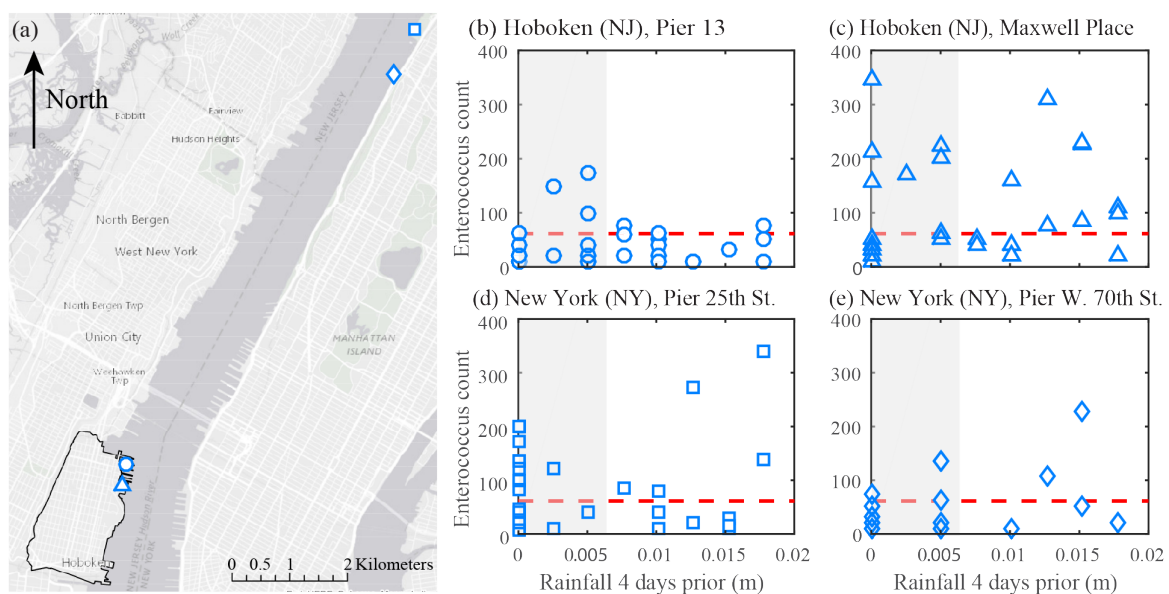


Figure 1. (a) Locations of water sampling along the Hudson River at four locations within the New York City metropolitan area; (b–e) FIB concentrations recorded between May 2014 and September 2016 [41]. The red line indicates the beach action value (BAV) concentration of 60 cells/100 mL of water, regulated by the U.S. EPA. The grey area in parts (b) through (e) indicates the dry-weather condition, i.e., rainfall less than 0.0063 m. The City of Hoboken is highlighted with a black contour.

Figure 2 shows the maps of the city plan, the geology [50], the elevation, the sewer network, and the location of the groundwater monitoring wells. All the visualization of the thematic maps was done using GIS software ArcGIS [51]. Additional details about the area are provided in the Supplementary Materials.

The exact age of the sewer is not known but best information is the major network was built prior to 1916 and no rehabilitation of the sewer mains have been done over the years. The system is combined and the material of the pipes varies between: brass, bricks, iron, concrete, clay, PVC,

and wood. Both circular and egg-shape pipes are present and foundations are mainly made of piles. As the sewer system was built long before the current wastewater treatment plant (WWTP), the sewer pipes run directly to the Hudson River. Around 1956, when the WWTP was built, an interceptor sewer was constructed along the river, which collects the flow from the various parts of the sewer network. At each point, a regulator with outfall was also built. The outfall was needed to direct combined sewage beyond the capacity of the system out to the river. There are currently five regulators with outfall in Hoboken (Figure 2b). A scheme of the regulator is reported in Figure S7b. Between regulators 4 and 5, an inline lifting plant is present that raises the wastewater from -2.3 to 8.8 m. Outfalls 4 and 5 are located at, respectively, -2.3 and 0.3 m (i.e., -7.4 and 1.0 ft) with respect to NAVD 88 datum. It has been an information from a personal correspondence with NHSA that the sewer system in Hoboken is affected indeed by large amount of infiltrations. A recent document [52] published by the authority reports measured infiltration that can be as large as 100% of the dry weather flow.

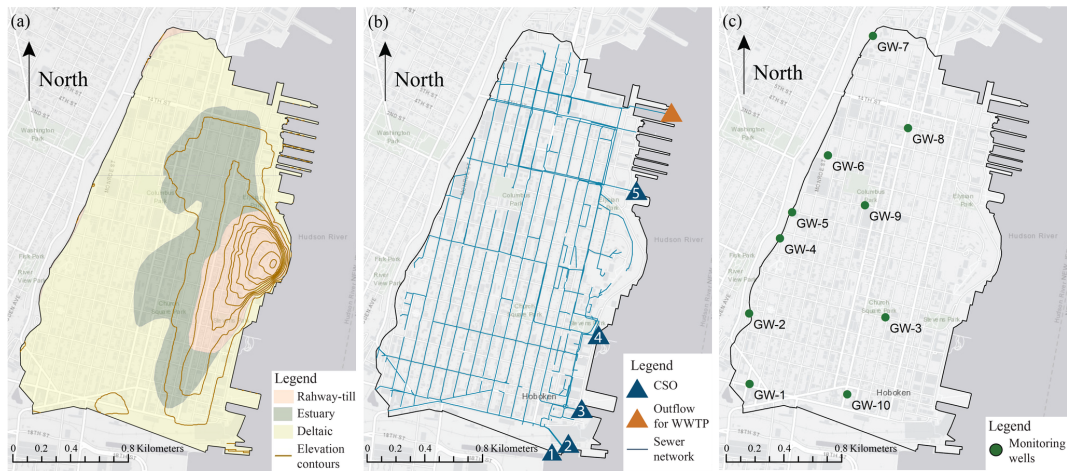


Figure 2. Maps of the study area showing: (a) the city plan with the shallow geology and the elevation [50]; (b) the sewer network with the outflows; and (c) the locations of the groundwater monitoring wells. The datum in parts (a) and (c) is NAVD 88. The map of the sewer system was provided by the North Hudson Sewerage Authority (NHSA).

Cracks along joints, within the bricks and at the connections, have been observed and CCTV images/movies also show infiltration of water (Figure 3).

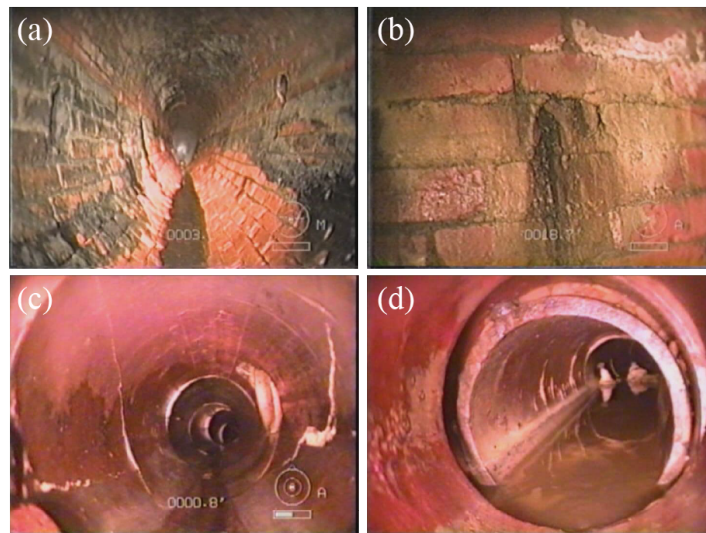


Figure 3. CCTV images of damaged pipes within the sewer network of Hoboken. (a,b) egg-shape conduit in bricks; (c,d) circular conduit in clay.

2.2. Sewer Flow Modeling

The flow in the sewer network was described using the U.S. EPA Storm Water Management Model (SWMM) [53], which is a hydrodynamic rainfall–runoff and urban drainage model widely used to simulate the hydrologic and stormwater components in urbanized areas [53–57].

The hydrologic module was used to determine from the rainfall the run-off, using the Manning’s equation, and infiltration into the ground, using the curve number method. In this work, the full dynamic wave flow routing option was used to account for the complex backwater effects and pressurized flow phenomena. The investigated area was approximately 3 km² and it was partitioned into 126 sub-drainage areas. As the southern part is characterized by large population density and low ground elevation, the sewer network in that area was described with a resolution higher than in the northern part of the city where a single conduit per sub-catchment was considered, instead. Figure 4 shows the scheme of the simulated sewer network. This approach with dual-resolution is not expected to affect the accuracy of the prediction of the total volumetric flow, as reported in the earlier work by Goldstein et al. [58].



Figure 4. Sewer network of the City of Hoboken as implemented in SWMM [53].

Dry-weather inflow was assumed only from residential areas and was averagely distributed to all of the manholes inside a sub-catchment. The flow rate in DWCs was calculated from the water consumption data within the city of Hoboken provided by the local Water Authority [59], as a total

annual consumption of 5.7 million m³ in 2016. The population in Hoboken was estimated to be 54,379 in 2016 [60] and, therefore, the average water consumption resulted to be equal to 11.90 L/h per inhabitant. The daily DWCs water consumption pattern was estimated by the indoor residential daily water usage pattern based on AWWARF residential end uses in the water report published in 1999 [61]. As 59% of the developed areas in the City of Hoboken is high density residential area with average garden size per unit less than 500 m² [62] (Figure 5a), no other water usage patterns were applied in the model. Figure 5b shows the resulting dry-weather flow pattern. The dry weather flow rate in each manhole Q_m was determined as,

$$Q_m = f_h \frac{AD_s Q_a}{n_m}, \tag{1}$$

where f_h is the factor of time pattern varies with hour, A is the area of sub-catchment, Q_a is the water consumption per capita per hour, n_m is the number of manhole in a sub-catchment, and D_s is the population density of a sub-catchment, which was converted from 2010 US census grid data [48].

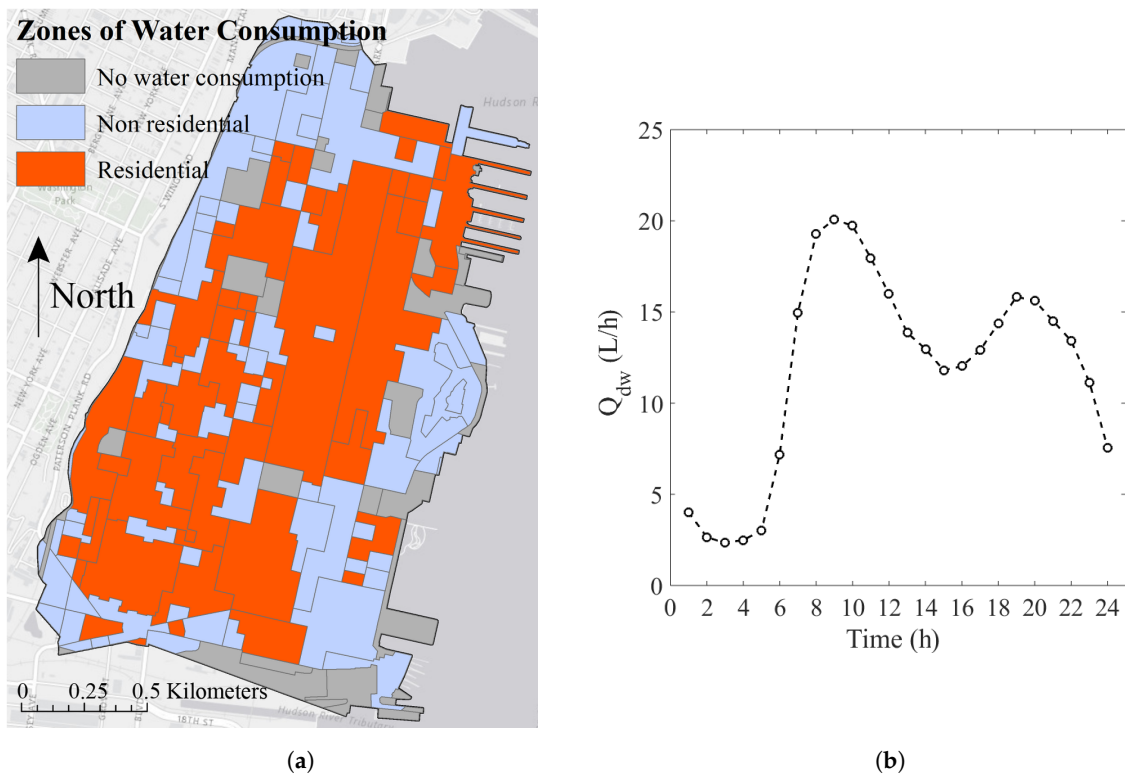


Figure 5. Information required for dry-weather flow calculations: (a) distribution of the land use; and (b) daily residential water discharge per capita.

The inputs in WWCs was based on the properties of the sub-drainage areas, which connect to the rest of the network through inlets. The imperviousness and average slope of the drainage areas was determined on the basis of the NJDEP land use dataset and NJDEP digital elevation model (DEM) [49,62,63]. The data of rain events were taken from the NASA database [64]. Further details regarding the sewer network and its implementation are reported in the Supplementary Materials. The model was validated in wet-weather conditions using measurements at five regulators [65] optimizing the CSO geometry and the pump curve. The damage of the sewer was not considered in the validation. Figure 6 shows the results. As it is possible to see, the model agrees very well with the data.

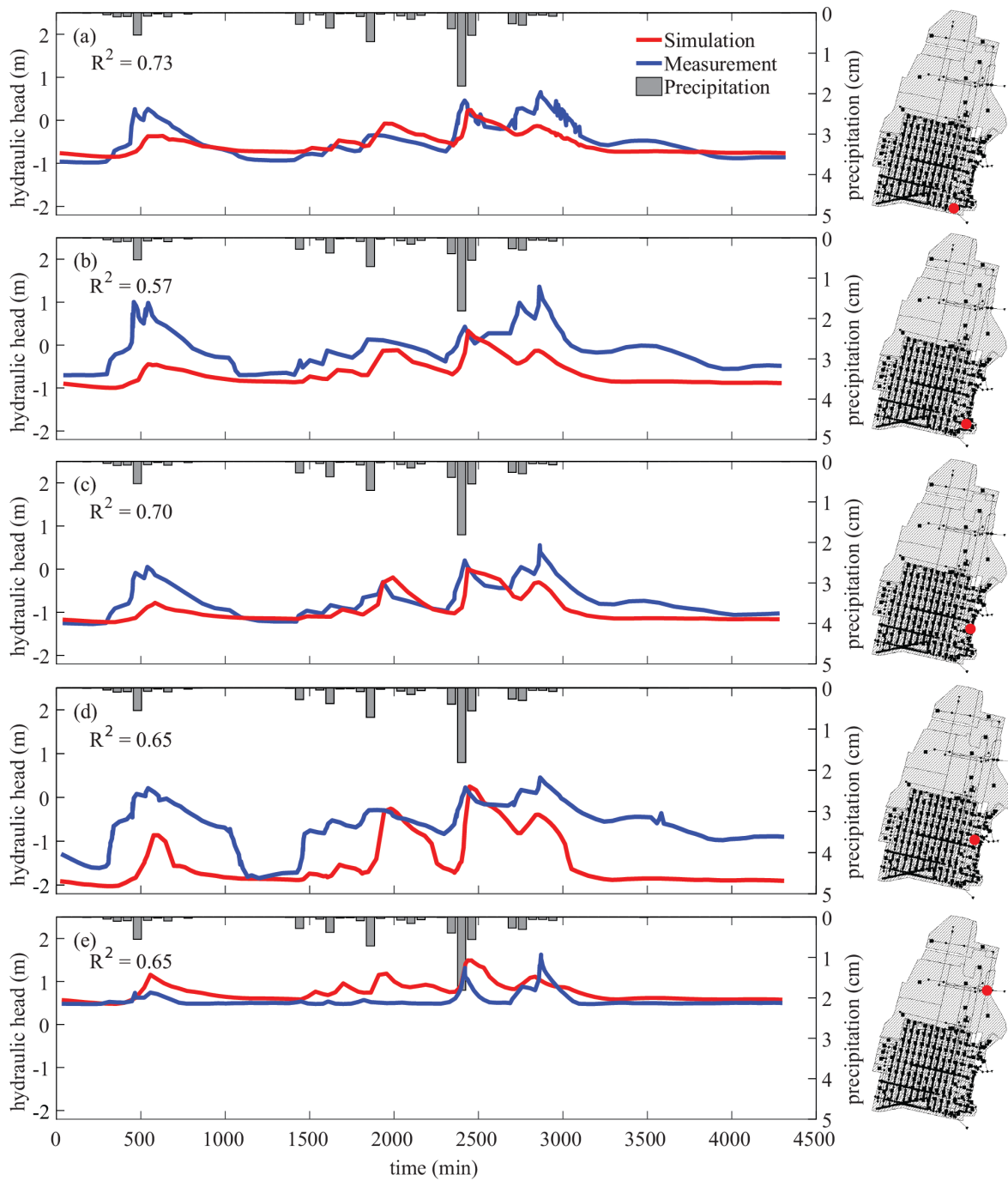


Figure 6. Validation of the sewer model in WWCs. The diagrams report the hydraulic head of the water within the pipe (solid lines) and precipitation depth. The measurements were carried out at five regulators indicated in the insets, from 17 May 2011 to 20 May 2011 [65]. (a–e) show the comparison of simulations with the measurements for, correspondingly, regulators 1 through 5.

2.3. Groundwater Flow Model

Groundwater flow simulations were carried out using the open-source software MODFLOW [66] with the interface provided by the Groundwater Modeling System (GMS) [67]. MODFLOW is a three dimensional (3D) finite difference model developed by the U.S. Geological Survey (USGS). The software was used to simulate the evolution of the water table within the study area of Hoboken. Four boundaries were identified of which three were inland and one at the shore. Data for the boundary conditions consist of the measurements of the: (1) water table at the observation wells; and (2) river

level at the tide measuring station [68]. Surface infiltration during wet weather may become a recharge for the shallow aquifer. However, the urban surface has an imperviousness exceeding 80% of its total extension, therefore, this recharge was neglected in this study.

The hydraulic conductivity (K , m/s) of the unconfined aquifer was determined using the one-dimensional hydraulic diffusivity equation [69,70] and resulted to be 0.63 ± 0.60 m/s. This value falls in the range of the typical hydraulic conductivity values for gravel [71]. However, the soil within the modeled aquifer is characterized predominantly by silty sand and fine gravel. Such a large value of the hydraulic conductivity could be due to the significant heterogeneity of the urban subsurface, where utilities and foundation are present. The domain shown in Figure 7 includes one single layer of 19,116 cells, of which 14,237 are active. The top of the layer corresponds to the ground morphology and the bottom is located at -13 m below datum, which corresponds to the deepest level at which geological information were available. Each cell has variable depth due to the variable altitude of the ground and a square flat base with a side of 15 m. For the boundary conditions (BCs), measurements of the water table of the shallow aquifer provided by the Municipality of Hoboken for the period between September 2015 and March 2016 were used. The measurements were performed in several monitoring wells within the city and along its boundary. Figure 8a shows the location of the wells and parts b through d report the corresponding dataset along the inland boundaries (purple, red, and black lines) upon averaging. Figure 8e shows the variation of the water level of the river during the period of the water table measurements. These data were downloaded from the public website of the National Oceanographic and Atmospheric Administration (NOAA) and correspond to the water level of the Hudson river at the Battery Park in New York City [68]. Each dataset at the inland boundaries was fitted by a Fourier series. The resulting functions were then used to describe the boundary conditions for the groundwater simulations. All data used for the boundary conditions are also shown in Figure S1. Further details regarding the geology, and the calculations of the hydraulic conductivity are provided in the Supplementary Materials.

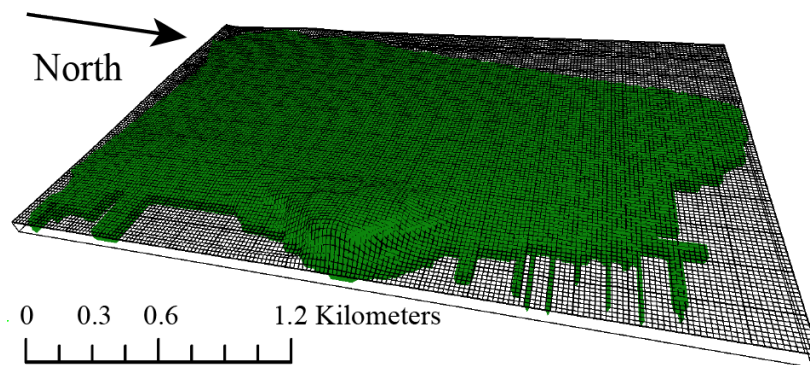


Figure 7. Domain of the aquifer of the City of Hoboken as implemented in MODFLOW [66].

The model was validated using transient dataset. For the simulations, the hydraulic conductivity was changed within its interval of uncertainty. The calculations were performed using the Time Variance package, which implements the stochastic parameter randomization. Figure 9 shows the results. In particular, the figure reports the calculated water table at the three observation wells within the domain, namely, GW 3, GW 8, and GW 9, located as shown in Figure 2. The shaded area in Figure 9 is bounded by the maximum and the minimum envelopes of the the calculated water table. As it is possible to see, the data fall within the interval of variation of the simulated water table, indicating that the measurements and the model agree well. Upon validation, groundwater flow simulations were performed for a total time of 190 days with a time interval of half-day and with initial head taken as steady state. The lowest river level for the initial state, i.e., 0.18 m above datum, was considered. The results were used to identify the location of water table of the unconfined aquifer underneath the City of Hoboken.

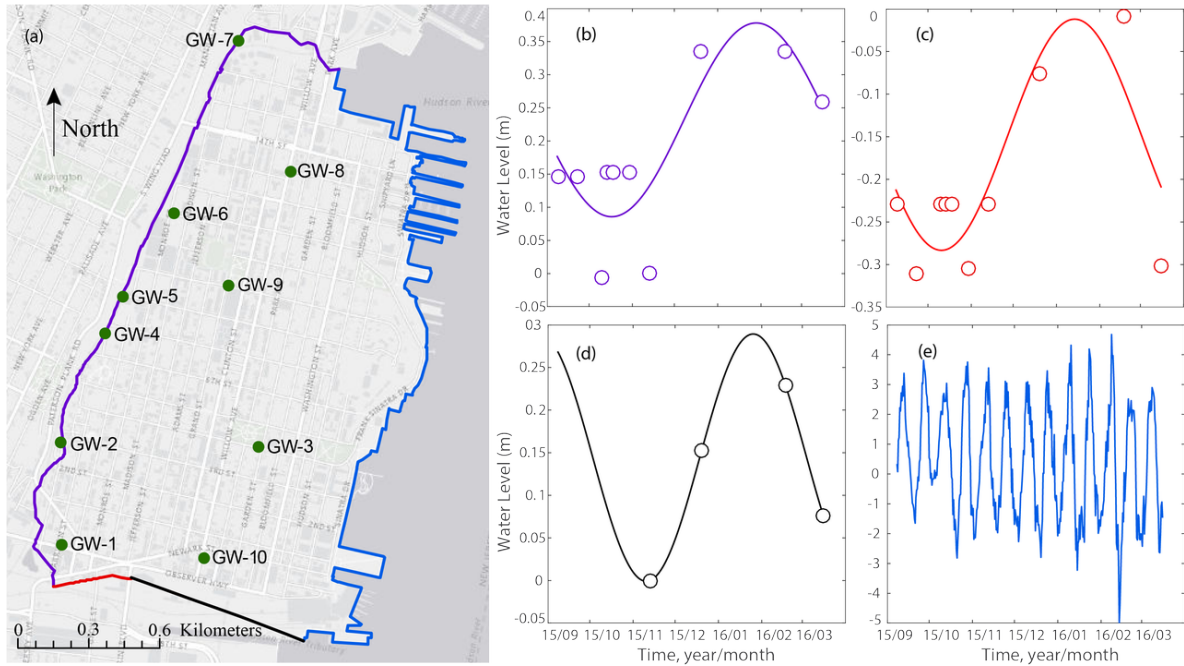


Figure 8. (a) Locations of the monitoring wells and identification of the boundaries for the groundwater model (datum NAVD 88); (b–d) values and interpolation of the water table data; and (e) Hudson River level at the Battery Park in New York City [68].

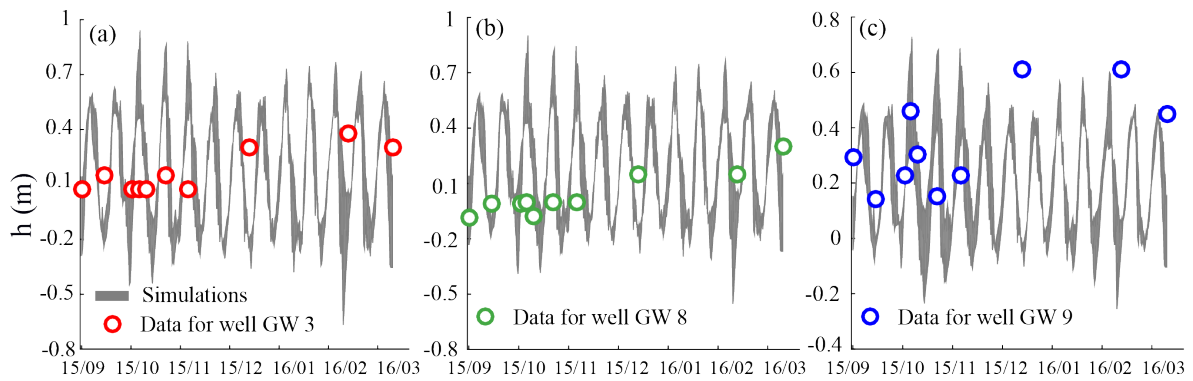


Figure 9. Validation of the groundwater model through stochastic simulations of the water table at three observation wells in Hoboken: (a) GW 3; (b) GW 8; and (c) GW 9.

2.4. Model of Risk of Failure and Infiltration

The sewer system is subjected to a significant structural stress because of aging, soil settlement, traffic load, tree roots, and extreme weather events [72,73]. Structural damages make the pipe pervious and potentially affected by infiltrations of groundwater, thereafter. In addition, infiltration may weaken the soil surrounding the pipe because of erosion [24].

In this section, a model combining risk of failure and risk of infiltration in a sewer network was developed. The failure risk model accounts for key influence factors of structural damage, as listed in Table 1, together with the corresponding coefficients of risk of failure (i.e., x) and relative weights (i.e., w). The values of x change between 0 and 1, with the largest value corresponding to the highest risk of failure. Figure 10 shows the thematic maps for each influence factor.

For each j -pipe, the risk of failure (RF) was determined as,

$$RF_j = \sum_{i=1}^{N=7} w_i x_{i,j}, \tag{2}$$

where the subscript i refers to an influence factor. The results of the sewer failure model using Equation (2) are shown in Figure 10h.

Table 1. Influence factors of structural damage of a sewer. The symbols x and w are the likelihood of failure and the relative weight coefficients.

| Influence Factor | x | Description | w |
|-----------------------|-----|---|------|
| Ductility | 0 | Flexible material. | 0.21 |
| | 0.5 | Rigid material. | |
| | 1 | Unknown material. | |
| Foundation/geology | 0 | Rock. | 0.18 |
| | 0.5 | Rahway-till. | |
| | 1 | Deltaic and estuarine deposit. | |
| Gradient | 0 | $0 < \text{slope} < 1.23$. | 0.07 |
| | 0.5 | $-0.0063 < \text{slope} < 0$. | |
| | 1 | $\text{slope} < -0.0063, \text{slope} > 1.22$. | |
| Joints | 0 | On-site built sewer. | 0.05 |
| | 0.5 | Pre-built elements or wood. | |
| | 1 | Unknown | |
| Traffic load | 0 | Low. | 0.15 |
| | 0.5 | Medium. | |
| | 1 | High. | |
| Groundwater (x_g) | 0 | Upstream and downstream manholes above the water table. | 0.24 |
| | 0.5 | Only one manhole is above the water table. | |
| | 1 | Upstream and downstream manholes below the water table. | |
| Size and shape | 0 | Egg-shape pipes. | 0.10 |
| | 0.5 | Circular pipes with $D \leq 0.38$ m. | |
| | 1 | Unknown or circular pipes with $D > 0.38$ m. | |

Including: ductile iron, PVC, and wooden pipe; Including: brass, brick, concrete, reinforced concrete, and vitrified clay pipe; Here, the reference is the shallow geology map. Pipes laying in two different geology formations are rated with the highest likelihood of failure; The distribution of the slopes of the conduits follows a normal distribution of mean value equal to -0.0063 ± 1.2345 with 95% confidence; Pipes in brick and wood were built on-site and they are continuous with joints only at the manhole; Pre-built elements of brass, concrete, reinforced concrete, ductile iron, PVC, and vitrified clay can have several joints within two manholes; No public transportation; Single public transportation route; Multiple public transportation routes; For the failure risk model the water table was considered equal to the average calculated level.

The risk of failure was combined with the results of the water table calculations to determine the risk of infiltration (RI) for a j -pipe as,

$$RI_j = x_{g,j}RF_j, \quad (3)$$

where $x_{g,j}$ is the likelihood of failure referring to groundwater influence factor (Table 1). RI was determined for each pipe within the network of Hoboken considering the shallowest and the deepest calculated water table.

2.5. Modeling Groundwater Infiltration into the Sewer System

The infiltration into the sewer was determined on the basis of the vertical distance of the invert level of the pipe and the water table, the surface area of the pipe, and the degree of damage of the pipe [74]. Infiltration (I) as excess water with respect to the dry weather flow (DWF) was considered for a certain portion of the sewer and 0 otherwise. The amount of infiltration was assumed within values reported in the literature as listed in Table 2. In the sewer model implemented in SWMM, the infiltration flow was added as direct inflow to the downstream manhole of each conduit with an infiltration risk of at least 50%.

Table 2. Summary of previous works where infiltration into a sewer network was quantified. The symbol *I* indicates the excess of water with respect to the dry weather flow.

| | Location | System Type | <i>I</i> |
|---|----------------------|-------------|-----------|
| Belhadj et al. [75] | Nante (France) | Separated | 0.73 |
| De Bénédictis and Bertrand-Krajewski [23] | Lyon (France) | – | 0.2 |
| Eiswirth and Houtzl [76] | Rastatt (Germany) | Separated | 1.08 |
| Kracht et al. [77] | Zurich (Switzerland) | Combined | 0.39 |
| Karpf et al. [78] | Dresden (Germany) | Separated | 0.33 |
| Prigiobbe and Giulianelli [25] | Rome (Italy) | Combined | 0.14–0.50 |
| Beheshti and Sægrov [79] | Trondheim (Norway) | Separated | 0.75 |

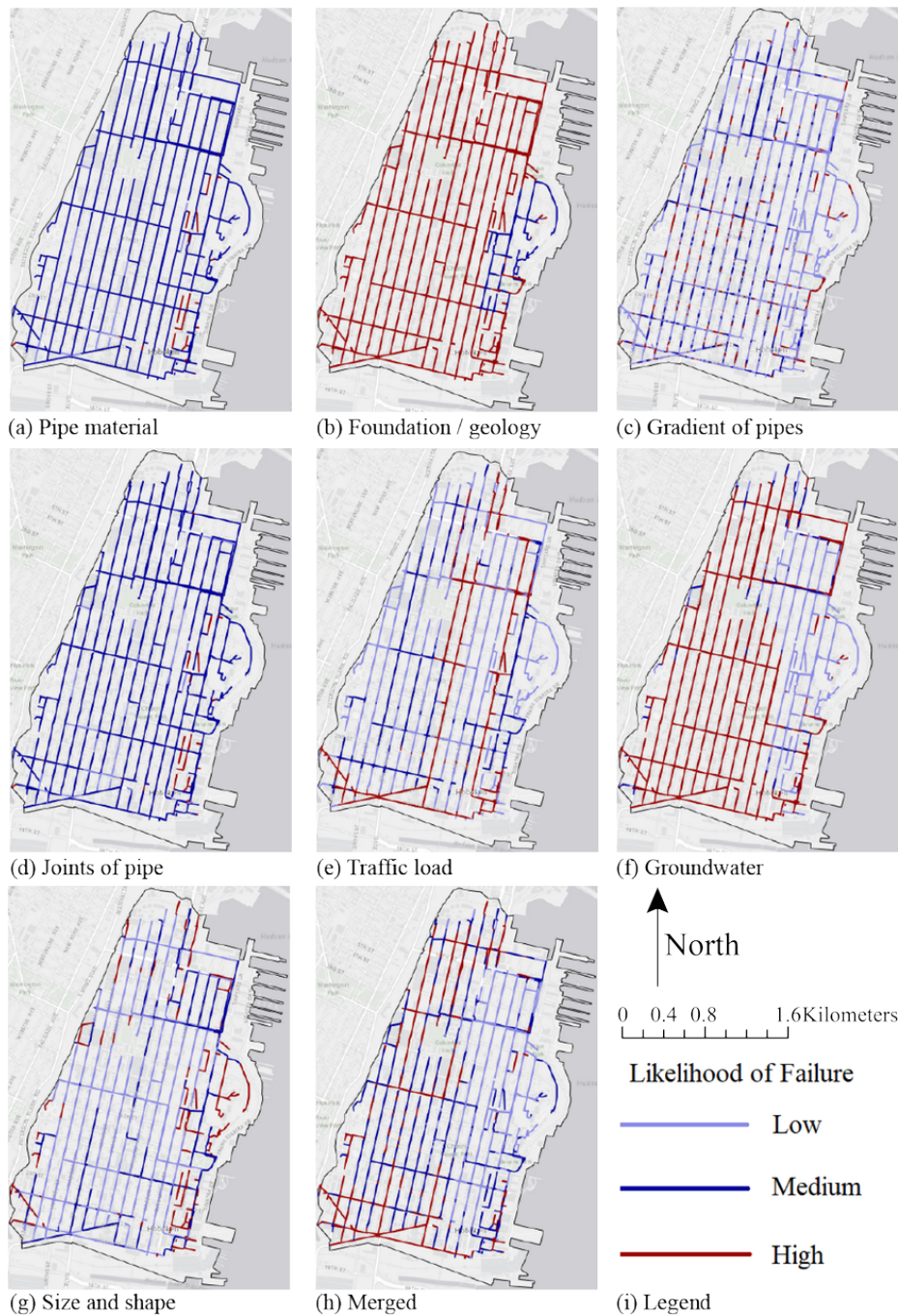


Figure 10. (a–g) influence factor distribution across the sewer network; and (h) results using Equation (2).

3. Results and Discussion

In this section, the results of the sewer and groundwater simulations in conjunction with the determination of risk of failure and infiltration are reported and discussed. First, the simulations from the hydrologic model of the sewer flow in dry weather were analyzed to verify the first hypothesis regarding the FIB events in DWCs, i.e., the sewer network is undersized. The dry-weather sewer flow simulation are performed without the presence of infiltration. The simulation results show that there is no flow at the CSOs (Figure S8) and no flooding at any catchments, which indicates the sewer system is not undersized under DWCs. Second, the calculations from the groundwater model are described and used to determine the risk of infiltration across the network. Finally, considering the sections of the sewer at high risk of infiltration, sewer flow simulations were run and the minimum level of infiltration required for the CSOs to occur in outfall 5 (Figure 2) was determined.

3.1. Sewer Flow Modeling

The results of the sewer flow simulations are reported in Figure 11 for the five outfalls and they are expressed as flow rate (Q) over time during a 72-h dry-weather period. The river level was considered equal to 0.13 m (0.44 ft) with respect to datum. This number corresponds to the average river level measured during the periods dry weather of the FIB events (i.e., between May 2014 and September 2016, shown Figure S1). As it is possible to see in Figure 11, no CSOs occur during DWCs, indicating that the sewer system in the City of Hoboken is not undersized.

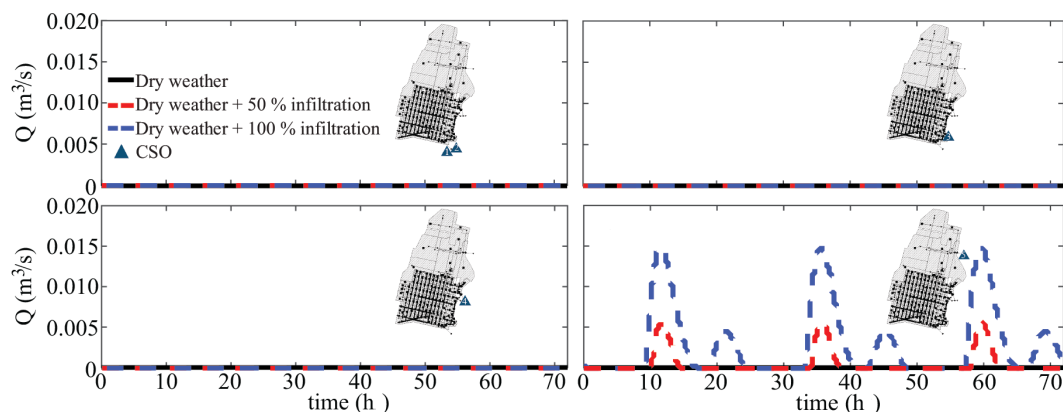


Figure 11. Flow rate as function of time at the five outfalls of the city of Hoboken in DWCs and DWCs with infiltrations. The simulated infiltration rate was set equal to 50% and 100% of the average dry-weather flow. The river level was fixed at 0.13 m above datum.

Simulations show that CSOs can activate upon a rain event with a hourly intensity equal to 1/3 of the intensity of one-year return period (Figure S8). This may explain the high FIB concentrations in Figure 1 after even a minor precipitation event.

3.2. Groundwater Modeling

The groundwater model was used to identify the location of the water table of the unconfined aquifer underneath the City of Hoboken. The simulations were run using the average calculated value of K , which is equal to 0.63 m/s and considering the lowest river level for the initial state, i.e., 0.18 m above datum. The boundary conditions were assumed as reported in Section 2.3. Figure 12 shows the results expressed as the smallest, the average, and the largest hydraulic head of the shallow aquifer. Here, it is possible to notice that the water table has a negligible change at the inland boundaries, varying 0.01–0.2 m with respect to datum. On the contrary, along the shore, the water table varies much more significantly changing between 0.7 and 1.5 m with respect to datum.

These results were combined with the failure risk model for the sewer network to identify the sections of the system with the largest risk of groundwater infiltration.

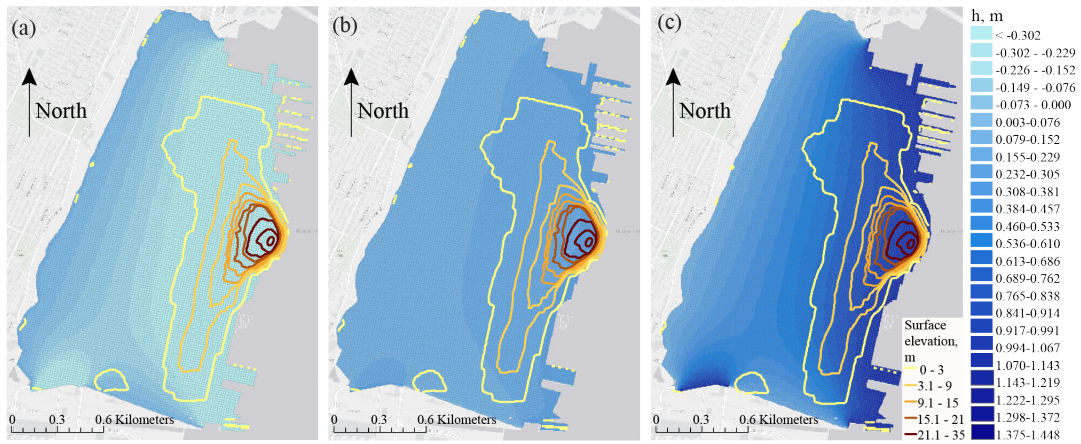


Figure 12. Simulation results of the water table of the unconfined aquifer underneath the City of Hoboken: (a) the deepest; (b) the average; and (c) the shallowest calculated levels with respect to datum.

3.3. Risk of Failure and Infiltration

The risk of failure (*RF*) was determined for the sewer network using Equation (2) and the results are shown in of Figure 10h. As it is possible to see, more than a half of the system has at least 47% likelihood of significant structural damage. As expected, these highly damaged pipes are located in the western side of the investigated area, where they are embedded in the weakest soil and below the average level of the groundwater. The risk of groundwater infiltration (*RI*) was calculated using Equation (3) by combining the results of the risk of failure with the results of groundwater model simulations. Figure 13 shows the distribution of *RI* across the network. Under the assumption of the shallowest water table, half of the network has more than 50% risk of infiltration. This is because a larger fraction of the network is submerged by the unconfined aquifer. Considering the deepest level of the water table (Figure 13b), the results do not change, because the portion of the submerged network is not significantly influenced by the tidal variation of the water table.

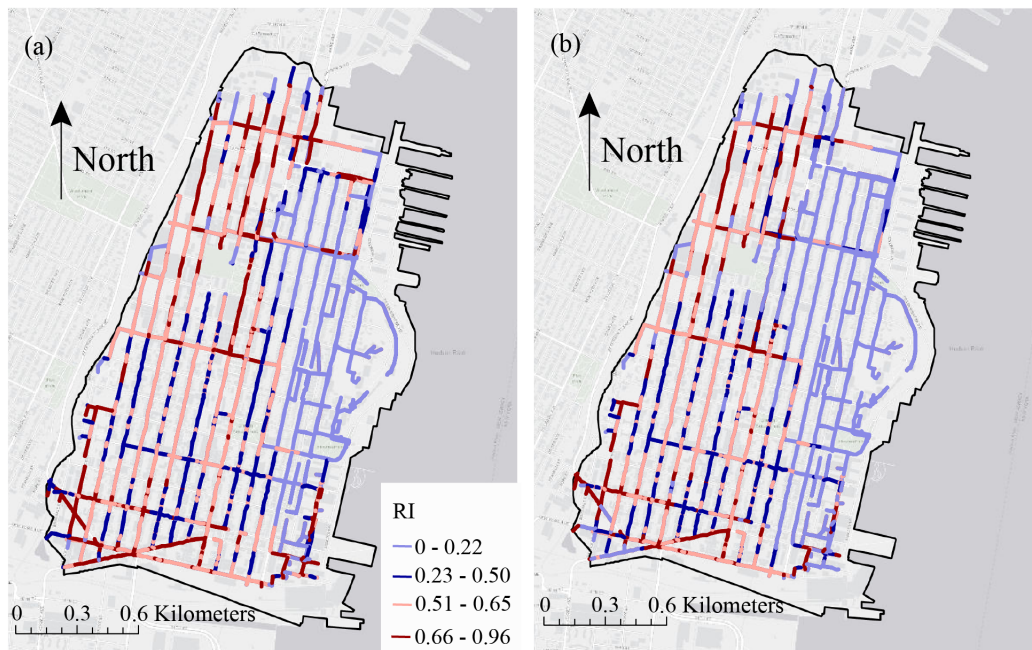


Figure 13. Map of the risk of groundwater infiltration (*RI*) considering: (a) the shallowest water table; and (b) the deepest water table.

3.4. Determination of the CSOs

To verify our second hypothesis of FIB events in DWCs, sewer flow simulations were performed considering infiltration occurring in the parts of the network with $RI \geq 51\%$. Infiltration was considered as an excess of water with respect to the dry-weather flow and the values were changed within the overall interval reported in the literature, as listed in Table 2. In Figure 11, it is possible to see that an amount of infiltration as large as 50%, which is much lower than the values measured by the Water Authority of the City of Hoboken [52], already activates outfall 5 in DWCs. Outfall 5 is located at the sampling location where FIB events in DWCs were observed (Figure 1c). This suggests that the FIB events in dry weather could indeed have been determined by the presence of additional water within the network entering the system through the damaged pipes submerged by the groundwater.

4. Conclusions

In this paper, a study of the potential causes of the occurrence of Fecal Indicator Bacteria (FIB) events in dry-weather conditions (DWCs) is presented. A hydraulic model of a sewer was implemented to understand if the sewer was undersized and a model combining sewer failure with groundwater level was developed to identify the sections potentially affected by infiltration. The results show that the risk of infiltration exceeds 50% of probability in almost a half of the entire network even at the lowest calculated water table. Considering 50% of infiltration distributed throughout that part of the network, CSOs can indeed occur also in DWCs.

Overall, this paper presents a study analyzing an emerging issue in coastal urban areas where sewer infrastructure is aging and low quality of surface water is observed in the nearby waterways. Considering the scenarios of sea-level rise [80–82], low-lying coastal areas may become even more vulnerable to groundwater infiltration into aging sewer systems in the near future. The paper provides a method to prioritize the renovation of sewer parts that not only are in an advanced stage of deterioration but also contribute to discharge untreated sewage into urban waterways.

Supplementary Materials: Supplementary Materials can be found at <http://www.mdpi.com/2073-4441/10/12/1774/s1>. Figure S1: (a) Dataset of Fecal Indicator Bacteria (FIB) concentration (*Enterococcus Faecalis* count per 100 mL) in the Hudson River at the two locations in Hoboken (NJ) as indicated in parts b and c of Figure 1 in the manuscript. (b) Rainfall depth. (c) Tidal river and water table elevations with respect to NAVD 88 datum. Figure S2: (a) Drainage areas built in detailed in SWMM. (b) Example of the location of the boundaries of the sub-catchments and their relationship with street blocks and surface runoff inlets. Figure S3: (a) Imperviousness as provided by NJDEP 2012 land use data. (b) Raster imperviousness converted from panel (a). (c) Average imperviousness assigned to the sub-catchments from the raster imperviousness layer. Figure S4: (a) Digital elevation model (DEM); (b) Slope rate calculated from DEM; (c) average slope rate assigned to sub-catchments from the raster slope layer. Figure S5: (a) Outfall; (b) Front view of the regulator. Figure S6: Flow rate as function of time at the five outfalls of Hoboken in both dry weather and wet weather conditions. The wet weather condition was selected as the minimum rain event at which CSOs occur, which corresponds to a 72-h rain event with peak hourly intensity equal to 1/3 of 1-year return period. Figure S7: Geology of Hoboken. (a) Shallow geology within the domain with boring log locations; (b) stratigraphy along the section A–A.

Author Contributions: T.L. implemented the sewer model and ran the simulations. X.S. implemented the groundwater model and ran the simulations. V.P. supervised the work. All three authors contributed to the writing of the manuscript.

Funding: This research received no external funding.

Acknowledgments: The authors would like to thank the Municipality of Hoboken and Dewberry Company for providing data of the water table and the North Hudson Sewerage Authority (NHSA) for giving the information and the maps of the sewer network. Moreover, the authors would like to thank: Firas Saleh at Jupiter (previously at Stevens Institute of Technology) for the technical support in the modeling of the sewer network using the software SWMM at the beginning of this work; Maryam Beheshti from Norwegian University of Science and Technology (NTNU) (Norway); and Martijn Kriebel and Robin Noordhoek from The University of Twente (Netherlands). Finally, the ASCE North Jersey Branch is gratefully acknowledged.

Conflicts of Interest: The authors declare no conflict of interest.

References

- Haase, D. Effects of urbanisation on the water balance—A long-term trajectory. *Environ. Impact Assess. Rev.* **2009**, *29*, 211–219. [[CrossRef](#)]
- Buhaug, H.; Urdal, H. An urbanization bomb? Population growth and social disorder in cities. *Glob. Environ. Chang.* **2013**, *23*, 1–10. [[CrossRef](#)]
- GHO. Global Health Observatory (GHO) Data. 2016. Available online: <http://apps.who.int/gho/data/node.home> (accessed on 29 November 2018).
- Rodriguez, C.; Van Buynder, P.; Lugg, R.; Blair, P.; Devine, B.; Cook, A.; Weinstein, P. Indirect Potable Reuse: A Sustainable Water Supply Alternative. *Int. J. Environ. Res. Public Health* **2009**, *6*, 1174–1209. [[CrossRef](#)] [[PubMed](#)]
- Brookes, K.; Brown, L.; Ruth, R. Transition to a water-cycle city: Risk perceptions and receptivity of Australian urban water practitioners. *Urban Water J.* **2014**, *11*, 427–443.
- Vázquez-Suñá, E.; Sánchez-Vila, X.; Carrera, J. Introductory review of specific factors influencing urban groundwater, an emerging branch of hydrogeology, with reference to Barcelona, Spain. *Hydrogeol. J.* **2005**, *13*, 522–533. [[CrossRef](#)]
- Brown, H. Eco-logical Principles for Next-Generation Infrastructure. *Bridge* **2011**, *41*, 19–26.
- Chen, J.; Theller, L.; Gitau, M.W.; Engel, B.A.; Harbor, J.M. Urbanization impacts on surface runoff of the contiguous United States. *J. Environ. Manag.* **2017**, *187*, 470–481. [[CrossRef](#)]
- Wen, Y.; Schoups, G.; van de Giesen, N. Organic pollution of rivers: Combined threats of urbanization, livestock farming and global climate change. *Sci. Rep.* **2017**. [[CrossRef](#)]
- Halliday, E.; Gast, R.J. Bacteria in Beach Sands: An Emerging Challenge in Protecting Coastal Water Quality and Bather Health. *Environ. Sci. Technol.* **2011**, *45*, 370–379. [[CrossRef](#)]
- Pachepsky, Y.A.; Shelton, D.R. Escherichia Coli and Fecal Coliforms in Freshwater and Estuarine Sediments. *Crit. Rev. Environ. Sci. Technol.* **2011**, *41*, 1067–1110. [[CrossRef](#)]
- Chen, G.; Walker, S.L. Fecal Indicator Bacteria Transport and Deposition in Saturated and Unsaturated Porous Media. *Environ. Sci. Technol.* **2012**, *46*, 8782–8790. [[CrossRef](#)]
- Russell, T.L.; Yamahara, K.M.; Boehm, A.B. Mobilization and Transport of Naturally Occurring *Enterococci* in Beach Sands Subject to Transient Infiltration of Seawater. *Environ. Sci. Technol.* **2012**, *46*, 5988–5996. [[CrossRef](#)] [[PubMed](#)]
- Schirmer, M.; Leschik, S.; Musolff, A. Current research in urban hydrogeology—A review. *Adv. Water Resour.* **2013**, *51*, 280–291. [[CrossRef](#)]
- Young, S.; Juhl, A.; O’Mullan, G.D. Antibiotic-resistant bacteria in the Hudson River Estuary linked to wet weather sewage contamination. *J. Water Health* **2013**, *11*, 297–310. [[CrossRef](#)]
- Phillips, P.; Schubert, C.; Argue, D.; Fisher, I.; Furlong, E.; Foreman, W.; Gray, J.; Chalmers, A. Concentrations of hormones, pharmaceuticals and other micropollutants in groundwater affected by septic systems in New England and New York. *Sci. Total Environ.* **2015**, *512–513*, 43–54. [[CrossRef](#)] [[PubMed](#)]
- McLellan, S.L.; Hollis, E.J.; Depas, M.M.; Dyke, M.V.; Harris, J.; Scopel, C.O. Distribution and Fate of *Escherichia coli* in Lake Michigan Following Contamination with Urban Stormwater and Combined Sewer Overflows. *J. Great Lakes Res.* **2007**, *33*, 566–580. [[CrossRef](#)]
- Morgan, D.; Xiao, L.; McNabola, A. Evaluation of combined sewer overflow assessment methods: Case study of Cork City, Ireland. *Water Environ. J.* **2017**, *31*, 202–208. [[CrossRef](#)]
- Edge, T.; Hill, S. Occurrence of antibiotic resistance in *Escherichia coli* from surface waters and fecal pollution sources near Hamilton, Ontario. *Can. J. Microbiol.* **2005**, *51*, 501–505. [[CrossRef](#)]
- Donovan, E.P.; Staskal, D.F.; Unice, K.M.; Roberts, J.D.; Haws, L.C.; Finley, B.L.; Harris, M.A. Risk of gastrointestinal disease associated with exposure to pathogens in the sediments of the Lower Passaic River. *Appl. Environ. Microbiol.* **2008**, *74*, 1004–1018. [[CrossRef](#)]
- USEPA. *The Clean Water and Drinking Water Gap Analysis*; United States Environmental Protection Agency: Washington, DC, USA, 2002.
- Koch, G.H.; Brongers, M.P.; Thompson, N.G.; Virmani, Y.P.; Payer, J.H. *Corrosion Cost and Preventive Strategies in the United States*; Technical Report, FHWA-RD-01-156; NACE International: Houston, TX, USA, 2002.
- De Bénédittis, J.; Bertrand-Krajewski, J.L. Infiltration in sewer systems: Comparison of measurement methods. *Water Sci. Technol.* **2005**, *52*, 219–227. [[CrossRef](#)]

24. Ellis, B.; Bertrand-Krajewski, J.L. *Assessing Infiltration and Exfiltration on the Performance of Urban Sewer Systems*; Technical Report; IWA Publishing: London, UK, 2010.
25. Prigiobbe, V.; Giulanelli, M. Quantification of sewer system infiltration using $\delta^{18}\text{O}$ hydrograph separation. *Water Sci. Technol.* **2009**, *60*, 727–735. [[CrossRef](#)] [[PubMed](#)]
26. Wittenberg, H.; Aksoy, H. Groundwater intrusion into leaky sewer systems. *Water Sci. Technol.* **2010**, *62*, 92–98. [[CrossRef](#)]
27. Karpf, C.; Krebs, P. Quantification of groundwater infiltration and surface water inflows in urban sewer networks based on a multiple model approach. *Water Res.* **2011**, *45*, 3129–3136. [[CrossRef](#)]
28. Beheshti, M.; Saegrov, S. Quantification Assessment of Extraneous Water Infiltration and Inflow by Analysis of the Thermal Behavior of the Sewer Network. *Water* **2018**, *10*, 1070. [[CrossRef](#)]
29. Phillips, P.J.; Chalmers, A.T.; Gray, J.L.; Kolpin, D.W.; Foreman, W.T.; Wall, G.R. Combined Sewer Overflows: An Environmental Source of Hormones and Wastewater Micropollutants. *Environ. Sci. Technol.* **2012**, *46*, 5336–5343. [[CrossRef](#)] [[PubMed](#)]
30. Granata, F.; Papirio, S.; Esposito, G.; Gargano, R.; de Marinis, G. Machine Learning Algorithms for the Forecasting of Wastewater Quality Indicators. *Water* **2017**, *9*, 105. [[CrossRef](#)]
31. Yap, H.T.; Ngien, S.K. Assessment on inflow and infiltration in sewerage systems of Kuantan, Pahang. *Water Sci. Technol.* **2017**, *76*, 2918–2927. [[CrossRef](#)]
32. Guo, S.; Yang, Y.; Zhang, Y. An approximate model on three-dimensional groundwater infiltration in sewer systems. *Water Sci. Technol.* **2017**, *75*, 306–312. [[CrossRef](#)]
33. Bondt, K.D.; Seveno, F.; Petrucci, G.; Rodriguez, F.; Joannis, C.; Claeys, P. Potential and limits of stable isotopes ($\delta^{18}\text{O}$ and δD) to detect parasitic water in sewers of oceanic climate cities. *J. Hydrol. Reg. Stud.* **2018**, *18*, 119–142. [[CrossRef](#)]
34. Yan, T.; Sadowsky, M.J. Determining Sources of Fecal Bacteria in Waterways. *Environ. Monit. Assess.* **2007**, *129*, 97–106. [[CrossRef](#)]
35. Panasiuk, O.; Hedström, A.; Marsalek, J.; Ashley, R.M.; Viklander, M. Contamination of stormwater by wastewater: A review of detection methods. *J. Environ. Manag.* **2015**, *152*, 241–250. [[CrossRef](#)] [[PubMed](#)]
36. Song, Q.; Zhao, M.R.; Zhou, X.H.; Xue, Y.; Zheng, Y.J. Predicting gastrointestinal infection morbidity based on environmental pollutants: Deep learning versus traditional models. *Ecol. Indic.* **2017**, *82*, 76–81. [[CrossRef](#)]
37. USGS. *Distribution of Fecal Indicator Bacteria along the Malibu, California, Coastline*; US Geological Survey: Reston, VA, USA, 2011.
38. Izbicki, J.; Swarzenski, P.; Reich, C.; Rollins, C.; Holden, P. Sources of Fecal Indicator Bacteria in Urban Streams and Ocean Beaches, Santa Barbara, California. *Ann. Environ. Sci.* **2009**, *3*, 139–178.
39. Philly-Rivercast. Philly Rivercast Water Quality Designations. 2017. Available online: <http://www.phillyrivercast.org/> (accessed on 29 November 2018).
40. Eleria, A.; Vogel, R.M. Predicting fecal coliform bacteria levels in the Charles River, Massachusetts, USA. *JAWRA* **2005**. [[CrossRef](#)]
41. HRECOs. Hudson River Environmental Conditions Observing System. Available online: <http://www.hrecos.org/> (accessed on 29 November 2018).
42. Leeming, R.; Bate, N.; Hewlett, R.; Nichols, P. Discriminating faecal pollution: A case study of stormwater entering Port Phillip Bay, Australia. *Water Sci. Technol.* **1998**, *38*, 15–22. [[CrossRef](#)]
43. Fan, J.; Ming, H.; Li, L.; Su, J. Evaluating spatial-temporal variations and correlation between fecal indicator bacteria (FIB) in marine bathing beaches. *J. Water Health* **2015**, *13*, 1029–1038. [[CrossRef](#)]
44. Tondera, K.; Klaer, K.; Roder, S.; Brueckner, I.; Strathmann, M.; Kistemann, T.; Schreiber, C.; Pinnekamp, J. Developing an easy-to-apply model for identifying relevant pathogen pathways into surface waters used for recreational purposes. *Int. J. Hyg. Environ. Health* **2016**, *219*, 662–670. [[CrossRef](#)] [[PubMed](#)]
45. Zimmer-Faust, A.G.; Thulsiraj, V.; Lee, C.M.; Whitener, V.; Rugh, M.; Mendoza-Espinosa, L.; Jay, J.A. Multi-tiered approach utilizing microbial source tracking and human associated-IMS/ATP for surveillance of human fecal contamination in Baja California, Mexico. *Sci. Total Environ.* **2018**, *640*, 475–484. [[CrossRef](#)]
46. Gao, G.; Falconer, R.A.; Lin, B. Modelling importance of sediment effects on fate and transport of *Enterococci* in the Severn Estuary, UK. *Mar. Pollut. Bull.* **2013**, *67*, 45–54. [[CrossRef](#)]
47. Wolf, L.; Eiswirth, M.; Hötzl, H. Assessing sewer-groundwater interaction at the city scale based on individual sewer defects and marker species distributions. *Environ. Geol.* **2006**, *49*, 849–857. [[CrossRef](#)]

48. *Census Blocks (2010) in New Jersey, Edition 20140523 (Govt_census_block_2010)*; US Census Bureau: Washington, DC, USA, 2010. Available online: https://www.state.nj.us/dep/gis/digidownload/metadata/statewide/Govt_census_group_2010.html (accessed on 29 November 2018).
49. NJDEP, 10-m Digital Elevation Grid of the Hackensack and Pascack Watershed Management Area (WMA 5). 2002. Available online: <https://www.nj.gov/dep/gis/wmalattice.html> (accessed on 29 November 2018).
50. Stanford, S.D. *Surficial Geology of the Elizabeth Quadrangle, Essex, Hudson, and Union Counties, New Jersey*; New Jersey Geological Survey: Trenton, NJ, USA, 2002.
51. Desktop, E.A. Release 10. *Redlands CA Environ. Syst. Res. Inst.* **2011**, 437, 438.
52. NHSA. System Characterization Report for the Adams Street WWTP. 2018. Available online: https://www.nj.gov/dep/dwq/pdf/CSO_SystemCharacterization_NHSAAdamsStreet_20180701.pdf (accessed on 29 November 2018).
53. Gironás, J.; Roesner, L.A.; Rossman, L.A.; Davis, J. A new applications manual for the Storm Water Management Model (SWMM). *Environ. Model. Softw.* **2010**, *25*, 813–814. [[CrossRef](#)]
54. Shrestha, N.K.; Leta, O.T.; De Fraine, B.; van Griensven, A.; Bauwens, W. OpenMI-based integrated sediment transport modelling of the river Zenne, Belgium. *Environ. Model. Softw.* **2013**, *47*, 193–206. [[CrossRef](#)]
55. Burger, G.; Sitzenfrei, R.; Kleidorfer, M.; Rauch, W. Parallel Flow Routing in SWMM 5. *Environ. Model. Softw.* **2014**, *53*, 27–34. [[CrossRef](#)]
56. Nanía, L.S.; León, A.S.; García, M.H. Hydrologic-hydraulic model for simulating dual drainage and flooding in urban areas: Application to a catchment in the metropolitan area of Chicago. *J. Hydrol. Eng.* **2014**, *20*, 04014071. [[CrossRef](#)]
57. Tian, Y.; Zheng, Y.; Wu, B.; Wu, X.; Liu, J.; Zheng, C. Modeling surface water-groundwater interaction in arid and semi-arid regions with intensive agriculture. *Environ. Model. Softw.* **2015**, *63*, 170–184. [[CrossRef](#)]
58. Goldstein, A.; Foti, R.; Montalto, F. Effect of Spatial Resolution in Modeling Stormwater Runoff for an Urban Block. *J. Hydrol. Eng.* **2016**, *21*, 06016009. [[CrossRef](#)]
59. Suez. *Your Water Quality Information. Consumer Confidence Report*; Technical Report; Suez: Paris, France, 2016.
60. US Census Bureau. *American FactFinder, Annual Estimates of the Resident Population: 1 April 2010 to 1 July 2016, 2016 Population Estimates*; US Census Bureau: Suitland, MD, USA, 2016.
61. Mayer, P.W.; DeOreo, W.B.; Opitz, E.O.; Kiefer, J.C.; Davis, W.Y.; Dziegielewski, B.; Nelson, J.O. *Residential End Uses of Water*; Technical Report; American Water Works Association Research Foundation and American Water Works Association: Denver, CO, USA, 1999. Available online: [https://www.waterdm.com/sites/default/files/WRF%20\(1999\)%20Residential%20End%20Uses%20of%20Water.pdf](https://www.waterdm.com/sites/default/files/WRF%20(1999)%20Residential%20End%20Uses%20of%20Water.pdf) (accessed on 29 November 2018).
62. *Land Use/Land Cover 2012 Update, Edition 20150217 Subbasin 02030101-Lower Hudson, Subbasin 02030103—Hackensack-Passaic (Land_lu_2012_hu02030101_103)*; NJ Department of Environmental Protection (NJDEP): Trenton, NJ, USA, 2015.
63. *Rebuild by Design-Hudson River Project, Hydrology and Flood Risk Assessment Report*; Technical Report; NJ Department of Environmental Protection (NJDEP): Trenton, NJ, USA, 2017.
64. NASA North American Land Data Assimilation System (NLDAS) Primary Forcing A Data. Site Code: NLDAS_FORA:X406-Y125. Technical Report. Available online: <https://ldas.gsfc.nasa.gov/nldas/NLDAS2forcing.php> (accessed on 14 February 2017).
65. City of Hoboken, NJ. Sewer Monitoring Program Observations and Data Analysis. Final Report. 15 November 2011. Technical Report. Available online: <https://www.jerseywaterworks.org/wp-content/uploads/2016/01/Hoboken-Emnet-Sewer-Monitoring-Study-2011-Final-Report.pdf> (accessed on 29 November 2018).
66. Harbaugh, A.; Banta, E.; Hill, M.; McDonald, M. *MODFLOW-2000, the U.S. Geological Survey Modular Groundwater Model User Guide to Modularization Concepts and the Groundwater Flow Process*; Technical Report; USGS: Reston, VA, USA, 2000.
67. *Groundwater Modeling System, Version 10.1*; AQUAVEO: Provo, UT, USA.
68. Oceanographic, N.; NOAA. The Battery, NY-Station ID: 8518750. Available online: <https://tidesandcurrents.noaa.gov/stationhome.html?id=8518750> (accessed on 14 February 2017).
69. Rotzoll, K.; El-Kadi, A.I. Estimating hydraulic properties of coastal aquifers using wave setup. *J. Hydrol.* **2008**, *353*, 201–213. [[CrossRef](#)]

70. Anderson, M.P.; William, W.; Woessner, R.J.H. *Applied Groundwater Modeling Simulation of Flow and Advective Transport*; Elsevier Inc.: Amsterdam, The Netherlands, 2015.
71. Freeze, R.; Cherry, J. *Groundwater*; 0-13-365312-9; Prentice-Hall: Upper Saddle River, NJ, USA, 1979.
72. Ariaratnam, S.T.; El-Assaly, A.; Yang, Y. Assessment of infrastructure inspection needs using logistic models. *J. Infrastruct. Syst.* **2001**, *7*, 160–165. [[CrossRef](#)]
73. Pikaar, I.; Sharma, K.R.; Hu, S.; Gernjak, W.; Keller, J.; Yuan, Z. Reducing sewer corrosion through integrated urban water management. *Science* **2014**, *345*, 812–814. [[CrossRef](#)]
74. Karpf, C.; Krebs, P. Sewers as drainage systems—quantification of groundwater infiltration. *Sustain. Tech. Strateg. Urban Water Manag.* **2004**, *2*, 969–975.
75. Belhadj, N.; Joannis, C.; Raimbault, G. Modelling of rainfall induced infiltration into separate sewerage. *Water Sci. Technol.* **1995**, *32*, 161–168. [[CrossRef](#)]
76. Eiswirth, M.; Houtz, H. The impact of leaking sewers on urban groundwater. *Groundw. Urban Environ.* **2006**, *1*, 399–404.
77. Kracht, O.; Gresch, M.; Gujer, W. A stable isotope approach for the quantification of sewer infiltration. *Environ. Sci. Technol.* **2007**, *41*, 5839–5845. [[CrossRef](#)]
78. Karpf, C.; Franz, T.; Krebs, P. Fractionation of infiltration and inflow (I/I) in urban sewer systems with regression analysis. In Proceedings of the NOVATECH 2007, Lyon, France, 24–28 June 2007; pp. 1227–1234.
79. Beheshti, M.; Sægrov, S. Sustainability assessment in strategic management of wastewater transport system: A case study in Trondheim, Norway. *Urban Water J.* **2018**, *15*, 1–8. [[CrossRef](#)]
80. Boon, J.D. Evidence of Sea Level Acceleration at U.S. and Canadian Tide Stations, Atlantic Coast, North America. *J. Coast. Res.* **2012**, *28*, 1437–1445. [[CrossRef](#)]
81. Ezer, T.; Atkinson, L.P. Accelerated flooding along the US East Coast: On the impact of sea-level rise, tides, storms, the Gulf Stream, and the North Atlantic Oscillations. *Earth Future* **2014**, *2*, 362–382. [[CrossRef](#)]
82. Krasting, J.P.; Dunne, J.P.; Stouffer, R.J.; Hallberg, R.W. Enhanced Atlantic sea-level rise relative to the Pacific under high carbon emission rates. *Nat. Geosci.* **2016**, *9*. [[CrossRef](#)]



© 2018 by the authors. Licensee MDPI, Basel, Switzerland. This article is an open access article distributed under the terms and conditions of the Creative Commons Attribution (CC BY) license (<http://creativecommons.org/licenses/by/4.0/>).